Electron, Positron, and Photon Wakefield Acceleration: Trapping, Wake Overtaking, and Ponderomotive Acceleration

T. Esirkepov, S. V. Bulanov, M. Yamagiwa, and T. Tajima

Kansai Research Establishment, JAEA, Kizu, Kyoto, 619-0215 Japan

(Received 20 April 2005; published 13 January 2006)

The electron, positron, and photon acceleration in the first cycle of a laser-driven wakefield is investigated. Separatrices between different types of the particle motion (trapped, reflected by the wakefield and ponderomotive potential, and transient) are demonstrated. The ponderomotive acceleration of electrons can be largely compensated by the wakefield action, in contrast to positrons and positively charged mesons. The electron bunch energy spectrum is analyzed. The maximum upshift of an electromagnetic wave frequency during reflection from the wakefield is obtained.

DOI: 10.1103/PhysRevLett.96.014803 PACS numbers: 41.75.Jv, 45.20.Jj, 52.38.Kd

Laser-driven charged particle acceleration is an attractive alternative to cyclic accelerators and linacs, promising to provide a much greater acceleration rate with a much more compact facility. At the dawn of laser technology, the electron acceleration with ''optical maser'' was suggested in Ref. [1]. In the laser wakefield accelerator (LWFA) concept introduced in Ref. [2], a long-living strong Langmuir wave (wakefield), induced by a short intense laser pulse in its wake in a low-density collisionless plasma, accelerates duly injected electrons. For efficient acceleration of charged particles, the laser pulse must be relativistically strong; i.e., its amplitude $a_0 = eE_0/m_e\omega c \gtrsim 1$. To provide electrons, one must use an externally preaccelerated electron bunch or exploit the effect of self-injection due to a longitudinal Langmuir wave break [3] or/and a transverse wave break [4].

Recent experiments [5,6] demonstrated localized energy spectra of electrons accelerated up to 170 MeV. The indications were given that the laser pulse underwent a self-focusing, and the wave breaking (both longitudinal and transverse) occurred in the first cycle of the wakefield and resulted in the electron self-injection.

Not only charged particles can get energy from the wakefield, but also photons. The wakefield is associated with an inhomogeneous electric charge density, moving with the wakefield phase velocity. An electromagnetic (EM) wave packet propagating in this medium undergoes a frequency shift due to the Doppler effect. In Ref. [7], a frequency upshift of the EM pulse copropagating with the wakefield was called ''photon acceleration.'' In the case of a counterpropagating EM pulse, the wakefield, close to wave breaking, can reflect a considerable amount of the pulse energy resulting in very high EM field intensification due to frequency upshift and focusing [8].

In a majority of publications on the LWFA, the periodical structure of the wakefield is implied. However, the laser-driven wakefield is not periodical, and a thorough analysis of its *first* cycle dynamics is of great importance. The first cycle can trap and accelerate an external electron bunch [9]. In Ref. [5], the localized electron energy spectrum was attributed to electrons that overtake the laser pulse due to acceleration in the wakefield first cycle. At the laser pulse front, conditions can be met for the so-called ''ponderomotive'' electron acceleration [10]. In this Letter, we present a general approach to the problem of acceleration of charged particles, electrons, and positrons, and photons in the *first* cycle of the wakefield.

In the framework of classical electrodynamics, the one-dimensional motion of a particle with charge $-e$ and mass m_e in the laser pulse and wakefield is described by the Hamiltonian $\mathcal{H} = \{m_e^2c^4 + c^2P_\parallel^2 + [cP_\perp + eA_\perp(x,t)]^2\}^{1/2} - e\varphi(x,t)$, where x is the particle coordinate, $P_\parallel$ and $P_\perp$ are components of the generalized momentum, $A_\perp$ is the laser pulse vector potential, and φ is the wakefield potential. If we neglect the laser pulse dispersion, then $A_\perp$ and φ depend on $X = x - v_g t$, where v_g is the laser pulse group velocity (equal to the wakefield phase velocity), $0 < v_g < c$. Thus, the Hamiltonian admits a Lie group with generators $v_g\partial_x + \partial_t$, ∂_y, ∂_z, and the Noether theorem implies three motion integrals: $\mathcal{H} - v_g P_\parallel = m_e c^2 h_0$, $P_\perp = P_{\perp 0}$, where h_0 and $P_{\perp 0}$ are constants of the particle initial state. To ensure the dependence of the Hamiltonian on $X = x - v_g t$, we assume that the laser pulse is circularly polarized and $P_{\perp 0} = 0$. We introduce dimensionless variables $\beta_{\rm ph} = v_g/c$, $\Phi(X) = e\varphi(X)/m_e c^2$, $p_x = P_\parallel/m_e c$, and $a(X) = eA_\perp(X)/m_e c^2$. In terms of new variables, the first integral gives the equation

$$h(X, p_x) \stackrel{\rm def}{=} \sqrt{1 + p_x^2 + a^2(X)} - \Phi(X) - \beta_{\rm ph} p_x = h_0. \quad (1)$$

According to its solution for $\beta_{\rm ph} < 1$, the particle moving from X_0 to X acquires the net kinetic energy

$$\mathcal{E} = \gamma_{\rm ph}^2(\Delta \pm \beta_{\rm ph}\{\Delta^2 - \gamma_{\rm ph}^{-2}[1 + a^2(X)]\}^{1/2}) - 1, \quad (2)$$

where $\gamma_{\rm ph} = (1 - \beta_{\rm ph}^2)^{-1/2}$, $\Delta = \Phi(X) + h_0$, and $p_{x0} = p_x(X_0)$; the sign ''+'' is for X increasing with time and ''$-$'' is for X decreasing with time.

To exemplify the general property of the system with Hamiltonian $h(X, p_x)$, we show its phase portrait in Figs. 1(c) and 1(d) for the electron with $P_{\perp 0} = 0$ in the case when the circularly polarized quasi-Gaussian laser pulse with amplitude $a(X) = a_0\{\exp[-4\ln(2)X^2/l_p^2] - 1/16\}\theta(l_p - |X|)$, where θ is the Heaviside step function [$\theta(\xi) = 1$ for $\xi \geq 0$ and $= 0$ for $\xi < 0$], $a_0 = 2$, FWHM size $l_p = 10$ wavelengths, propagating in an ideal hydrogen plasma with density $n_e = 0.01 n_{\rm cr}$, excites a wakefield, whose potential $\Phi(X)$ is described by the Poisson equation

$$\Phi'' = k_p^2 \gamma_{\rm ph}^3 \beta_{\rm ph}\{(1+\Phi)[\gamma_{\rm ph}^2(1+\Phi)^2 - 1 - a^2(X)]^{-1/2} - (\mu - \Phi)[\gamma_{\rm ph}^2(\mu-\Phi)^2 - \mu^2 - a^2(X)]^{-1/2}\}, \qquad (3)$$

where the prime denotes differentiation with respect to the X coordinate, $k_p = \omega_{pe}/c$, and $\mu = m_i/m_e = 1836$ is the ion-to-electron mass ratio. The potential, longitudinal electric field, laser pulse envelope, and the electron and ion densities are shown in Figs. 1(a) and 1(b), where X is normalized on the laser wavelength λ_L. We choose the finite quasi-Gaussian pulse shape to emphasize the existence of the ponderomotive separatrix (see below).

Each orbit $\{X(t), p_x(t)\}$ of the electron in the (X, p_x) plane is a segment of a level curve of the function $h(X, p_x)$. The (X, p_x) plane is divided into basins of a finite motion, where the particle is trapped by the wakefield potential, and two basins of infinite motion. The basins are separated from each other by special orbits, separatrices, which join at singular points situated on the curve $p_{xs}(X) = \beta_{\rm ph}\gamma_{\rm ph}[1 + a^2(X)]^{1/2}$. On this curve, the square root in the right-hand side of Eq. (2) vanishes: $[\Phi(X) + h_0]^2 - \gamma_{\rm ph}^{-2}[1 + a^2(X)] = 0$.

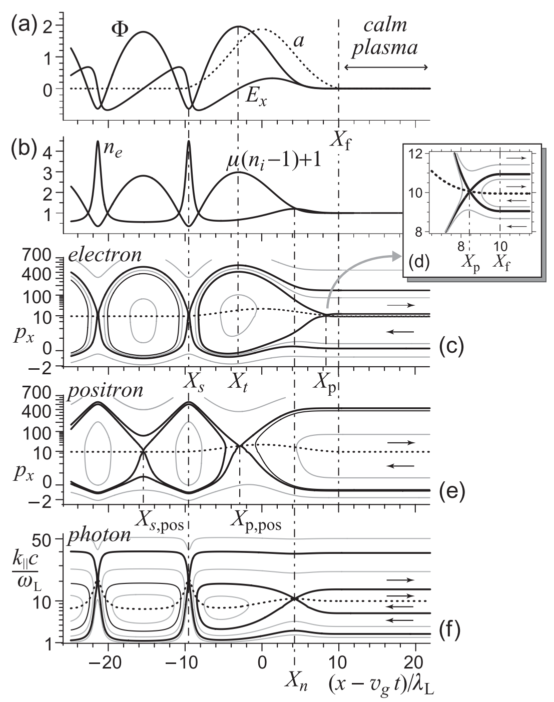

FIG. 1. (a) The wakefield excited by the laser pulse; (b) normalized electron and scaled ion density. Phase portrait for the (c) electron, (e) positron, and (f) photon. (d) The electron ponderomotive basin close-up. The thick solid line is for separatrices, the thin solid line for other orbits; the thick dotted line in (c) and (e) is for $p_x = \beta_{\rm ph}\gamma_{\rm ph}[1 + a^2(X)]^{1/2}$ and in (f) is for $k_\parallel c = \beta_{\rm ph}\gamma_{\rm ph}\omega_{pe}(X)$.

An electron started from the singular point X_s acquires the maximum kinetic energy at the top X_t of the separatrix. If the laser pulse length is shorter than half of wakefield wavelength, $l_p < \lambda_{\rm wf}/2$, then in the first cycle of the wakefield the points X_s and X_t correspond, respectively, to the local minimum and maximum of the wakefield potential, $\Phi(X_s) = \Phi_{\min}$, $\Phi(X_t) = \Phi_{\max}$. So the maximum kinetic energy on the separatrix is

$$\mathcal{E}_{\rm m} = \gamma_{\rm ph}^2\{\Delta\Phi_{\rm m} + \beta_{\rm ph}[\Delta\Phi_{\rm m}^2 + 2\gamma_{\rm ph}^{-1}\Delta\Phi_{\rm m}]^{1/2}\} + \mathcal{E}_0, \quad (4)$$

where $\Delta\Phi_{\rm m} = \Phi_{\max} - \Phi_{\min}$, $\mathcal{E}_0 = \gamma_{\rm ph} - 1$. If $\gamma_{\rm ph} \gg 1$, we have $\mathcal{E}_{\rm m} \approx 2\gamma_{\rm ph}^2\Delta\Phi_{\rm m} + \gamma_{\rm ph} - 1$. The lowest value of the potential Φ is reached when the laser pulse sweeps the greatest possible amount of electrons, $\Phi_{\min} \geq -1 + 1/\gamma_{\rm ph}$, and the highest value is limited by the ion response, $\Phi_{\max} \leq \mu(1 - 1/\gamma_{\rm ph})$. Knowing the minimum of the solution to Eq. (3), one can find its maximum; in the case of a sufficiently short and intense laser pulse ($l_p \ll \lambda_{\rm wf}$, $a \gg 1$), Eq. (3) gives $\Phi_{\max} = (1 - \gamma_{\rm ph}^{-1})(2\gamma_{\rm ph}\mu + \mu - 1)/(2\gamma_{\rm ph} + \mu - 1)$. If the laser pulse has the optimal length, then $\Phi_{\max} \approx a^2/2$ for $a \lesssim \sqrt{\mu}$ [11].

Since the laser pulse has a finite duration, the "runaway" separatrix exists, a segment of the level curve $h(X, p_x) = 1/\gamma_{\rm ph} - \Phi_{\min}$ [Fig. 1(c)]. If an electron beam is injected exactly onto this separatrix, it asymptotically *overtakes* the laser pulse and becomes monoenergetic with the final energy, as it follows from Eq. (4),

$$\mathcal{E}_{\rm f} = \gamma_{\rm ph}^2\{|\Phi_{\min}| + \beta_{\rm ph}[\Phi_{\min}^2 + 2\gamma_{\rm ph}^{-1}|\Phi_{\min}|]^{1/2}\} + \mathcal{E}_0, \quad (5)$$

where $|\Phi_{\min}| = -\Phi_{\min} > 0$. In the limit $\gamma_{\rm ph} \gg 1$, this energy can be much higher than the required minimum injection energy. If, additionally, the wakefield is strongly nonlinear ($a \gg 1$), $\Phi_{\min}$ tends to its lowest value $-1 + 1/\gamma_{\rm ph}$, and we have $\mathcal{E}_{\rm f,max} = 2\gamma_{\rm ph}^2 - 2$.

In the first cycle of the wakefield, behind the laser pulse there is also the "confining" separatrix, a segment of the level curve $h(X, p_x) \approx 1/\gamma_{\rm ph}$ (the exact value is discussed below). It encloses a basin of orbits of electrons which are trapped inside the potential well moving along with the laser pulse. Between the confining and runaway separatrices lie a bunch of reflecting orbits. On such an orbit, an electron starts with the longitudinal momentum p_x^- in the range $\beta_{\rm ph}\gamma_{\rm ph} > p_x^- > \beta_{\rm ph}\gamma_{\rm ph} + \gamma_{\rm ph}^2(\beta_{\rm ph}|\Phi_{\min}| - [\Phi_{\min}^2 + 2\gamma_{\rm ph}^{-1}|\Phi_{\min}|]^{1/2}) \geq 0$ at $t \to -\infty$. Then it is accelerated by the first cycle of the wakefield, reaching the maximum energy defined by Eq. (2), where one must substitute $X_0 = +\infty$, $p_{x0} = p_x^-$, $a(X_0) = \Phi(X_0) = 0$. Finally, the electron overtakes the laser pulse. Its longitudinal momentum p_x and kinetic energy $\mathcal{E}$ increase as

$$p_x^+ = p_x^- + 2\gamma_{\rm ph}^2\Gamma^-(\beta_{\rm ph} - v_x^-), \tag{6}$$

$$\mathcal{E}^+ = \mathcal{E}^- + 2\beta_{\rm ph}\gamma_{\rm ph}^2\Gamma^-(\beta_{\rm ph} - v_x^-) < \mathcal{E}_{\rm f}; \tag{7}$$

$\Gamma^- = [1 + (p_x^-)^2]^{1/2}$, $\mathcal{E}^- = \Gamma^- - 1$, $v_x^- = p_x^-/\Gamma^- < \beta_{\rm ph}$. The same equations describe an elastic rebound of a relativistic particle from the wall moving at a speed $\beta_{\rm ph}$.

Yet another, the third, ponderomotive separatrix exists in the vicinity of the laser pulse front $X_f = l_p$ [Figs. 1(c) and 1(d)]. It joins the second, confining, separatrix at the point $(X_{\rm p}, p_{xs}(X_{\rm p}))$ defined by the equation $a(X_{\rm p})a'(X_{\rm p}) = \gamma_{\rm ph}\Phi'(X_{\rm p})[1 + a^2(X_{\rm p})]^{1/2}$, and so the exact value of the Hamiltonian for both separatrices is $h_{\rm p} = h(X_{\rm p}, p_{xs}(X_{\rm p}))$. The third separatrix encloses a thin basin of orbits with $1/\gamma_{\rm ph} < h(X, p_x) < h_{\rm p} = h(X_{\rm p}, p_{xs}(X_{\rm p}))$, going from $X = +\infty$ at $t \to -\infty$ with $p_x < \beta_{\rm ph}\gamma_{\rm ph}$ and reflecting back with increased $p_x > \beta_{\rm ph}\gamma_{\rm ph}$ at $t \to +\infty$. In contrast to orbits between the confining and runaway separatrices, where particles are reflected by the wakefield potential, the orbits enclosed by the third separatrix belong to electrons which are reflected by the *ponderomotive force* of the laser pulse. Such reflection is possible because the laser pulse has the speed $v_g < 1$ and the wakefield potential $\Phi(X)$ always grows slower than the $a(X)$ on the laser pulse front. Using series expansions of $a(X)$ and $\Phi(X)$ about the point $X = X_f$, we can estimate the ponderomotive basin thickness, which is the energy difference between the upper and lower branches of the ponderomotive separatrix: at $|a'(X_f)| \ll 1$, and $\mu \gg 1$, $\gamma_{\rm ph} \gg 1$, $\mathcal{E}_{\rm p}^+ - \mathcal{E}_{\rm p}^- = 2\beta_{\rm ph}\gamma_{\rm ph}^2[h_p^2 - \gamma_{\rm ph}^{-2}]^{1/2} \approx -2\sqrt{3}\beta_{\rm ph}k_p^{-1}a'(X_f)\gamma_{\rm ph}^{1/2}$, where $\mathcal{E}_{\rm p}^- \approx \mathcal{E}_{\rm p}^+ \approx \gamma_{\rm ph} - 1$. The ponderomotive force is able to reflect only those electrons that move in the same direction as the laser pulse and whose velocity is slightly less than $\beta_{\rm ph}$. The energy gain is rather small because the ponderomotive and electrostatic potentials almost completely compensate each other. However, it is still not zero even with the ideal Gaussian pulse; the maximum effect is reached when the laser pulse has a sharp front: $\mathcal{E}_{\rm p}^+ - \mathcal{E}_{\rm p}^- = 2\beta_{\rm ph}\gamma_{\rm ph}a_0$. For a particle, initially at rest, the energy gain cannot be greater than $2\beta_{\rm ph}^2\gamma_{\rm ph}^2$ or $a_0^2/2$.

We examine the energy spectrum change of an electron bunch injected into the first cycle of the wakefield wave onto the runaway separatrix [Fig. 1(c)]. When a relatively long, initially quasi-monoenergetic, bunch is injected from the singular point X_s and accelerated in the first cycle of the wakefield wave, its particles are distributed along the runaway separatrix with some density $\mathcal{N}(X)$. As a result, the particle energy spectrum broadens from the initial energy $\mathcal{E}_0$ to the cutoff (maximum) energy $\mathcal{E}_m$. Besides these two limits, the spectrum has a peculiarity at $\mathcal{E}_{\rm f}$ (Fig. 2). Near the top of the separatrix, the particle energy has a parabolic dependence on X, $\mathcal{E}(X) \simeq \mathcal{E}_m[1 - (X - X_t)^2/l_{\rm acc}^2]$, where $l_{\rm acc} \approx \gamma_{\rm ph}^2\lambda_{wf}$ is the acceleration length

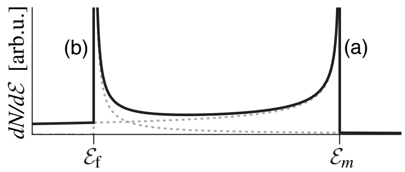

FIG. 2. The energy spectrum of the electron bunch: contributions from (a) particles scattered about the top of the separatrix and (b) particles that overtake the laser pulse.

[2]. Hence, the energy spectrum of particles collected over the wakefield period contains the following contribution from particles with energy near the cutoff energy:

$$\frac{dN}{d\mathcal{E}}\bigg|_{\mathcal{E}\to\mathcal{E}_m - 0} = \frac{\mathcal{N}(X)}{|d\mathcal{E}/dX|} \simeq \frac{\mathcal{N}(X_t)l_{\rm acc}}{2\sqrt{\mathcal{E}_m(\mathcal{E}_m - \mathcal{E})}}, \tag{8}$$

where $\mathcal{E} < \mathcal{E}_m$. If electrons are injected also onto separatrices in the other cycles of the wakefield, the resulting energy spectrum contains a superposition of peaks (8). If the particles are arranged uniformly on the separatrix, the spectrum, despite its (integrable) singularity, has a rather large spread; e.g., half of the particles occupy the energy interval $3\mathcal{E}_m/4 \le \mathcal{E} < \mathcal{E}_m$. A contribution to the spectrum from particles overtaking the laser pulse can be obtained from the dependence Eq. (2). Taking, for simplicity, the model dependence $\mathcal{E} = \mathcal{E}_f[1 + \delta\exp(-X/X_f)]$, $\delta = \text{const} > 0$, we obtain

$$(dN/d\mathcal{E})_{\mathcal{E}\to\mathcal{E}_f + 0} \simeq \mathcal{N}(X_f)X_f/(\mathcal{E} - \mathcal{E}_f). \tag{9}$$

In addition to the case of a negatively charged particle (electron), we consider the case of a positively charged particle (positron) [Fig. 1(e)]. The formulas (1) and (2) remain valid with the substitution $\Phi \to -\Phi$. In the wakefield, the electron's points of equilibrium correspond to the positron's singular points (for a sufficiently short laser pulse). The positron injected from the singular point into the second cycle of the wakefield returns back to the same singular point. In the first half-cycle of the wakefield, in contrast to the case of the electron, both forces acting on the positron—the wakefield electrostatic force and the laser pulse ponderomotive force—pull the positron in the same direction (forward). Therefore, we see a wide ponderomotive basin, where particles with initial momentum $\beta_{\rm ph}\gamma_{\rm ph} > p_{x,{\rm pos}}^- > \gamma_{\rm ph}^2(\beta_{\rm ph}\Delta_{\rm pos} - [\Delta_{\rm pos}^2 - \gamma_{\rm ph}^{-2}]^{1/2})$ are accelerated up to the energy

$$\mathcal{E}_{\rm p,pos}^+ = \gamma_{\rm ph}^2\{\Delta_{\rm pos} + \beta_{\rm ph}[\Delta_{\rm pos}^2 - \gamma_{\rm ph}^{-2}]^{1/2}\}, \tag{10}$$

in accordance with Eqs. (2) and (7). Here $\Delta_{\rm pos} = \Phi_{\rm p,pos} + \gamma_{\rm ph}^{-1}[1 + a_{\rm p,pos}^2]^{1/2}$, and the values $\Phi_{\rm p,pos}$ and $a_{\rm p,pos}$ are taken at the singular point $X_{\rm p,pos}$, a nontrivial solution to the equation $a(X)a'(X) + \gamma_{\rm ph}\Phi'(X)[1 + a^2(X)]^{1/2} = 0$. In the limit $\gamma_{\rm ph} \gg 1$, Eq. (10) becomes $\mathcal{E}_{\rm p,pos}^+ = 2\gamma_{\rm ph}^2\Phi_{\rm p,pos} + 2\gamma_{\rm ph}[1 + a_{\rm p,pos}^2]^{1/2}$. As the wakefield potential $\Phi(X)$ always grows slower than the laser amplitude $a(X)$, the contribution of the ponderomotive mechanism to the positron energy can be significant. The momentum of the lower branch of the ponderomotive separatrix is negative at $\Delta_{\rm pos} > 1$; thus, the positron initially at rest is accelerated up to momentum $2\beta_{\rm ph}\gamma_{\rm ph}^2$ and energy $2\beta_{\rm ph}^2\gamma_{\rm ph}^2$, in accordance with Eqs. (6) and (7). We see that even the "background" positrons, introduced externally or created in the laser-plasma interaction, are substantially accelerated, if $\Phi_{\rm p,pos} \gtrsim 1$. To ensure this effect in the case of more heavy particles, e.g., pions, the laser amplitude must be sufficiently large, $a_0 > \sqrt{m_\pi/m_e}$. In the limit of a long laser pulse ($l_p \gg \lambda_{\rm wf}$), also considered in Ref. [12], the maximum energy (10) becomes $\approx (1+\beta_{\rm ph})\gamma_{\rm ph}^2 a_0$, since $\Phi_{\rm p,pos} \approx a_0$ in this limit.

A sufficiently short EM pulse propagating in the wakefield-modulated plasma can be described in the geometric optics approximation as a particle ("photon") with coordinate x (center of the pulse) and momentum $\mathbf{k}$ (wave vector) by the Hamiltonian represented by the dispersion relation $\omega(x, \mathbf{k}; t) = [k^2c^2 + \omega_{pe}^2(x - v_{\rm ph}t)]^{1/2}$, $k^2 = k_\parallel^2 + k_\perp^2$. As in the case of the electron, the dependence on time and space only via $X = x - v_{\rm ph}t$ allows us to describe the photon by the Hamiltonian

$$\Omega(X, k_\parallel) = \sqrt{k_\parallel^2 c^2 + \omega_{pe}^2(X)} - \beta_{\rm ph} k_\parallel c \qquad (11)$$

and constant transverse momentum $k_\perp = k_{\perp 0}$ (we assume $k_{\perp 0} = 0$ for simplicity). The phase portrait of the photon is similar to that of the electron [see Fig. 1(f), where $k_\parallel c$ is normalized on the laser frequency ω_L]. We see the runaway and confining separatrices, as well as a ponderomotivelike basin, which corresponds to the photon reflection at the first maximum of the electron density piled up at the laser pulse front. (We notice that, when the wakefield is excited by an electron bunch, the phase portrait of the photon can be topologically equivalent to that of the positron.) On an orbit corresponding to the Hamiltonian value $\Omega(X, k_x) = \Omega_0 = \omega_0 - \beta_{\rm ph} k_{\parallel 0} c$, the photon frequency is

$$\omega = \gamma_{\rm ph}^2 \Omega_0 \{1 \pm \beta_{\rm ph}[1 - \omega_{pe}^2(X)\Omega_0^{-2}\gamma_{\rm ph}^{-2}]^{1/2}\}. \qquad (12)$$

A photon ($k_{\parallel 0}$, ω_0) that reflects from the first or second density peak (i.e., a photon in the ponderomotive basin or between the confining and runaway separatrices) undergoes frequency upshift $\tilde\omega = (2\gamma_{\rm ph}^2 - 1)\omega_0 - 2\beta_{\rm ph}\gamma_{\rm ph}^2 k_{\parallel 0} c$. Maximum frequency $\tilde\omega_{\rm max}$ of the photon reflected from the wakefield is the frequency on the runaway separatrix at $X \to +\infty$. The runaway separatrix corresponds to $\Omega_0 = \hat\omega_{pe}/\gamma_{\rm ph}$, where $\hat\omega_{pe} = \omega_{pe}(X_s)$ is the maximum plasma frequency (at the maximum plasma density); thus, from Eq. (12) we obtain

$$\tilde\omega_{\rm max} = \gamma_{\rm ph}\hat\omega_{pe}\{1 + \beta_{\rm ph}[1 - \omega_{pe0}^2/\hat\omega_{pe}^2]^{1/2}\}; \qquad (13)$$

$\omega_{pe0} = \omega_{pe}(+\infty)$ is the unperturbed plasma frequency. For $\hat\omega_{pe} \gg \omega_{pe0}$ and $\beta_{\rm ph} \to 1$, $\tilde\omega_{\rm max} \approx 2\gamma_{\rm ph}\hat\omega_{pe}$. A sufficiently strong wakefield can reflect a counterpropagating photon, $k_{\parallel 0} < 0$. In the limit $\omega_0 \gg \omega_{pe0}$, such a photon acquires frequency $\tilde\omega = \omega_0(1+\beta_{\rm ph})/(1-\beta_{\rm ph})$, the Einstein formula for the frequency of the EM wave reflected at a relativistic mirror in vacuum. The Einstein formula and Eq. (13) together impose the upper limit on the reflected photon frequency. The geometric optics approximation fails when the wakefield is close to wave breaking; nevertheless, the reflectance can be considerable [8].

In conclusion, in the first cycle of the Langmuir wave in the wake of a short relativistically strong laser pulse, at least three separatrices exist: On the runaway separatrix, the electron overtakes the wakefield and the laser pulse; on the confining separatrix, it moves together with the laser pulse; and the ponderomotive separatrix encloses a domain of the ponderomotive acceleration. The ponderomotive acceleration can significantly contribute to the energy gain of positrons and positively charged mesons, in contrast to electrons, for which it can be largely compensated by the wakefield action. The energy spectrum of the initially monoenergetic electron bunch accelerated in the wakefield first cycle has a typical shape with two peaks; the shape of the peak can indicate an acceleration mechanism. The upper limit on the frequency upshift of the EM wave reflected from the wakefield is obtained in the geometric optics approximation. Although the presented description is one-dimensional, revealed properties are present in three-dimensional configurations in the vicinity of the axis, where particles are most efficiently accelerated.

We thank the MEXT and CREST for their support.

[1] K. Shimoda, Appl. Opt. **1**, 33 (1962).
[2] T. Tajima and J. M. Dawson, Phys. Rev. Lett. **43**, 267 (1979).
[3] S. V. Bulanov *et al.*, JETP Lett. **53**, 565 (1991); S. V. Bulanov *et al.*, Phys. Fluids B **4**, 1935 (1992); C. A. Coverdale *et al.*, Phys. Rev. Lett. **74**, 4659 (1995); D. Gordon *et al.*, *ibid.* **80**, 2133 (1998); A. Zhidkov *et al.*, Phys. Rev. E **69**, 035401(R) (2004).
[4] S. V. Bulanov *et al.*, Phys. Rev. Lett. **78**, 4205 (1997); T. V. Liseikina *et al.*, Phys. Rev. E **60**, 5991 (1999); A. Pukhov and J. Meyer-ter-Vehn, Appl. Phys. B **74**, 355 (2002).
[5] S. P. D. Mangles *et al.*, Nature (London) **431**, 535 (2004).
[6] C. G. R. Geddes *et al.*, Nature (London) **431**, 538 (2004); J. Faure *et al.*, *ibid.* **431**, 541 (2004).
[7] S. C. Wilks *et al.*, Phys. Rev. Lett. **62**, 2600 (1989).
[8] S. V. Bulanov *et al.*, Phys. Rev. Lett. **91**, 085001 (2003).
[9] A. G. Khachatryan *et al.*, Phys. Rev. ST Accel. Beams **7**, 121301 (2004).
[10] A. V. Gaponov and M. A. Miller, Sov. Phys. JETP **34** 751 (1958); E. A. Startsev and C. J. McKinstrie, Phys. Plasmas **10**, 2552 (2003); S. Masuda *et al.*, *ibid.* **12**, 013102 (2005).
[11] S. V. Bulanov *et al.*, JETP Lett. **50**, 198 (1989).
[12] C. Du and Z. Xu, Phys. Plasmas **7**, 1582 (2000).